Journal of Power Sources 267 (2014) 731–738

Contents lists available at ScienceDirect

Journal of Power Sources

journal homepage: www.elsevier.com/locate/jpowsour

Laminar flow-based micro fuel cell utilizing grooved electrode surface

Seung-Mo Ha, Yoomin Ahn*

Dept. of Mechanical Engineering, Hanyang University, 55 Hanyangdaehak-ro, Sangnok-gu, Ansan, Gyeonggi-do 426-791, Republic of Korea

HIGHLIGHTS

- Electrode patterned with grooves is proposed for passive control of depletion zone.
- The depleted layer is recharged by a chaotic flow generated by the electrode pattern.
- Groove height and gap between the electrodes are optimized.
- The efficacy of the grooved pattern is increased when the electrode is long.
- Power density of grooved electrode is improved compared to that of a flat electrode.

ARTICLE INFO

Article history:
Received 28 March 2014
Received in revised form
1 June 2014
Accepted 2 June 2014
Available online 10 June 2014

Keywords:
Microfluidic fuel cell
Membraneless fuel cell
Grooved electrode surface
Depletion boundary layer
Advection
Cell performance

ABSTRACT

Microfluidic fuel cells have low power density and poor fuel utilization due to the generation of a reaction depletion zone. In this study, cell electrodes patterned with grooves are proposed for passive control of the depletion zone, where a secondary transport flow over the grooved electrode replenishes the depleted layers. The proposed membrane-less fuel cell is composed of a polydimethylsiloxane layer over a photoresist microchannel wall and a glass substrate that contains platinum electrodes. The optimum gap between the electrodes and the height of grooves are designed based on a computational fluid dynamics simulation. Hydrogen peroxide is used both as a fuel (when it is mixed with sodium hydroxide) and as an oxidant (when it is mixed with sulfuric acid). During the experiments, electrodes of various lengths are integrated on the bottom of the Y-channel. Experimental results show that the effect of grooves on cell performance is independent of fuel rate and fuel concentration, but the effect is remarkable when the length of the electrode is large. The peak power density with grooved electrodes improves by a maximum of 13.93% compared to that of planar electrodes. This grooved electrode-based fuel cell is expected to be a useful microdevice for power generation.

1. Introduction

Fuel and oxidant streams flow without turbulence when they are injected into the microchannel of a microfluidic fuel cell, and a liquid–liquid interface forms between the fuel and oxidant. As a result, a microfluidic fuel cell can easily solve problems inherent to the proton exchange membrane fuel cell (PEMEC). Also, since an expensive membrane is not necessary, the fabrication process becomes simple, and the production cost can be reduced [1]. Various types of fuels and oxidants and several materials for the electrode, catalyst, and electrolytes have been investigated to improve the power density of the microfluidic fuel cell [2–6]. It is difficult, however, to commercialize microfluidic fuel cells because their power density is still insufficient. During the operation of a microfluidic fuel cell, a reaction depletion zone and inter-diffusion zone appear in the microchannel flow. The reaction depletion zone occurs on the surface of the electrode, where by-products undergo an oxidation–reduction reaction with the fuel and oxidant, preventing continuous oxidation–reduction reactions at each of the electrodes [7].

The depletion boundary layer deteriorates the performance of the microfluidic fuel cell, and methods to control this phenomenon have been reported. Yoon et al. [8] arranged multiple inlets along the channel in the form of electrodes installed in the channel wall, and they refreshed the depletion zone by supplying fresh fuel and oxidants. In another setup, they placed many outlets along the channel wall and discharged the depleted fuel and oxidants many times to prevent accumulation over the electrodes. These sorts of active control methods increase power requirements because additional injection or emission and control of many fluids can be complicated. These disadvantages can be remediated through passive control methods. For example, they equipped a passive

* Corresponding author. Tel.: +82 31 400 5281; fax: +82 31 436 8146.
E-mail address: ahnym@hanyang.ac.kr (Y. Ahn).

http://dx.doi.org/10.1016/j.jpowsour.2014.06.005
0378-7753/

micromixer with herringbone ridge patterns at the base of the channel and made an exchange at the depletion zone with new fuel and oxidants through advection. The inter-diffusion zone in the center of the microchannel can be amplified by the mixer inside the channel; however, this can cause undesirable fuel crossover [9]. Another passive control method for suppression of the depletion zone expansion was proposed by Lim et al. [10]. They made a number of separate electrodes in the same direction as the flow of the fuel and oxidant in order to recharge the fuel and oxidant to their original concentrations in the gap between electrodes. Power density was somewhat reduced as a result of the non-electrode parts that exist in the channel, though [9]. Further, a flow-through porous anode electrode has been used as a smooth way to replenish the fuel depletion zone. This method provided good results when the flow rates of the fuel and electrolyte were medium to low [11,12]. On the other hand, an adjunctive mixing channel structure is needed to effectively pump fuel through the porous electrode. Flow resistance through the electrode brings a higher pressure drop, so a higher fuel injection power may be required.

Two or more fluids injected into a microchannel do not mix well due to the characteristics of laminar flow. In biochips, which use a microchannel, the process of mixing and reacting a variety of fluids is frequently essential. A micromixer, which blends the fluids within the microchannel, has been an important area of research in the microfluidics field. Stroock [13] et al. made herringbone ridges on the bottom of the microchannel and published information on a passive micromixer, which needs no additional apparatus to operate the mixer for the first time. Afterwards, many researchers have reported on micromixers utilizing diverse slant grooved structures [14–17]. This is because external equipment, such as a pump, valve, or pneumatic actuator is not necessary in these types of passive micromixers. Further, fabrication is comparatively easy among the micromixers that have been proposed up to now, but mixing efficiency is high and applications are varied.

To prevent stagnation of products created by the oxidation–reduction reaction of the fuel and oxidant on the electrode surfaces, i.e., to reduce the thickness of depletion boundary layer, flows on the electrode surface toward the fuel layer above the depletion zone must be produced. A passive micromixer is the simplest method to achieve this. On the contrary, other methods employing external equipment or additives, such as microbeads, are not suitable for inducing the mixed flow over the electrode surface within the microchannel, considering the operating principle of the device and the efficiency of the energy generated using the microfluidic fuel cell [18–21].

This study presents a microfluidic fuel cell that has grooved electrodes as a passive control method for the reaction depletion zone. A flow field is developed over the electrode surface using a grooved pattern to improve the power density and electrode surface area. Using software for computational fluid dynamics, the microfluidic fuel cell was designed to have an optimum height in the groove of the electrodes. By using an optimum design, liquid flow occurs in order to effectively lessen the thickness of the depletion layer on the electrode surfaces without affecting the inter-diffusion zone. The fuel cell that was designed is composed of a glass substrate on which a metallic thin film of grooved electrodes is deposited. Furthermore, a microchannel layer made of photoresist and a polydimethylsiloxane (PDMS) layer for the inlet and outlet are formed. Microfluidic fuel cells were fabricated with grooved electrodes and with general planar electrodes for a comparative experiment. The effects of the fuel concentration, flow rate, and length of the electrodes on the cell performance were investigated. The efficiency of the grooved electrode with respect to the improvement in the power density was analyzed.

2. Materials and methods

2.1. Design of the microfluidic fuel cell

A membrane-less fuel cell was designed to have a Y-shaped microchannel with electrodes on the base plane of the microchannel. The microchannel has an outlet and two inlets, and the width and height of the microchannel were set to 1.0 mm and 50 μm, respectively, using the previously reported characteristics of microfluidic fuel cells as a reference [9]. The length of the electrodes was then set to three different possible lengths of 20, 30, and 40 mm, and the microchannel was 2.2 mm longer than the electrode in all cases. In addition, the dimensional design of the fuel cell progressed in the order of the width of the electrode, the gap between the electrodes, and the height of the groove on the electrode surface. The mixing inside the microchannel was analyzed using the commercial fluid dynamics program CFD-ACE^{+} (ESI Group, France) for the design, and the analysis was based on the simple concentration transport equation and the Navier-Stokes equation of fluid dynamics. The zone to be analyzed was modeled with a 3-dimensional structured grid, and the number of total volumes and total nodes were 4 and 19,950, respectively. The flow module and user scalar module were used. A numerical analysis technique was used for the velocity field, and the upwind scheme was used with respect to the space difference in the enthalpy analysis. Squared conjugate gradient and preconditioning (CGS + Pre) were used in the calculation method. This method was also used for the calculation of the pressure field. The two injected fluids were assumed to be of deionized water for the computer aided analysis, and the assumed density and viscosity were 997 kg m^{-3} and 0.000855 kg m^{-1} s^{-1}, respectively. In this simulation, pressure at the two inlets was set at 10,000 N m^{-1}, so the fuel and oxidant were injected into the two inlets of the Y-shaped microchannel, each at a flow rate of about 0.1 m s^{-1}.

2.2. Microdevice fabrication

The microfluidic fuel cell was fabricated as shown in Fig. 1. It consisted of grooved electrodes, a microchannel, inlets for fuel and oxidant, and outlets. The fuel cell is made up of three primary layers: a lower glass substrate, a middle photoresist thick film, and an upper PDMS sheet. The anode and cathode electrodes are made

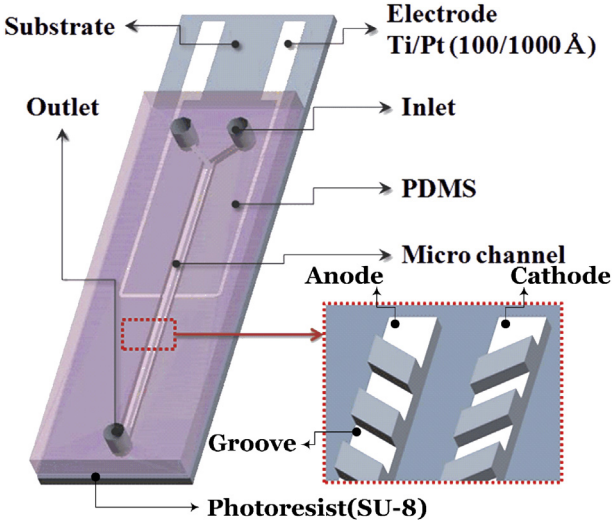

Fig. 1. Schematic diagram of proposed microfluidic fuel cell.

directly on the glass substrate, which then becomes the bottom of the microchannel. On top of that, a negative photoresist structure, which serves as the right and left walls of the microchannel, is formed. The PDMS sheet works as a cover for the microchannel. Polydimethylsiloxane is a transparent and highly elastic polymer, and it is a suitable material for the micro molding technique because of its low price and good formability. The microdevice was fabricated using the existing fabrication technique of a glass-PDMS hybrid microfluidic chip [22].

The lift-off technique was used to make the electrodes on the glass substrate. A positive photoresist (AZ5214E, Microchemicals GmbH, Germany) was spin-coated on a glass wafer (Pyrex 7740, Corning, USA), and then the parts at which the electrodes would be built were removed using photolithography. To eliminate the small amount of photoresist scum that had not been removed after processing of the spin-coated photoresist, a de-scum processing was carried out with O_2 plasma dry etching. Metallic thin films of 10 nm Ti and 100 nm Pt were then deposited in order using e-beam evaporation. Platinum film does not adhere well to a glass substrate. Good adherence of Pt for Ti coated glass has been reported [23]. Titanium was used as an adhesion layer to improve the bonding strength between the Pt film and the glass substrate and to enhance resistance against fluid flow erosion. By dipping the deposited films in acetone and organic solvents, the remainder of the metallic films (except for the electrode) was removed. After the flat electrodes were made, the groove pattern bumps were made by performing the lift-off process once more. The titanium adhesion layer was also used in the second metallic layer patterning stage, as in the first stage. Then, a negative photoresist (SU-8 3035, Micro-Chem Corp., USA) was spin-coated, and the microchannel was made through the photolithography process. Next, PDMS (Sylgard 184, silicon elastomer base, Dow Corning, USA) mixed with curing agent (Sylgard 184, silicon elastomer curing agent, Dow Corning, USA) at ratio of 10:1 was poured over the mold, and it was hardened at 65 °C for 4 h. Hardened PDMS was then separated from the mold, and inlets and outlets were made using mechanical punching. In order to integrate the finished PDMS layer to the SU-8 photoresist of the glass substrate, the surfaces of the PDMS and SU-8 photoresist were treated with O_2 plasma and then bonded with each other.

2.3. Experimental set-up

Fuel used for the microfluidic fuel cell was prepared by dissolving the same concentration of H_2O_2 (0.25, 0.5, 0.75 M) in a dilute NaOH (0.25, 0.5, 0.75 M) solution at a ratio of 1:1. As an oxidant, 0.25, 0.5, and 0.75 M H_2O_2 was dissolved in dilute 0.125, 0.25, and 0.375 M H_2SO_4 solutions, at the same ratio, respectively. The ratios of viscosity to density for H_2O_2, NaOH (50% purity), H_2SO_4 are about 0.858, 23.47, 14.51 $\times$ 10^{-6} m^2 s^{-1}, respectively, compared with 0.888 $\times$ 10^{-6} m^2 s^{-1} for deionized water used in the simulation. The Reynolds number is inversely proportional to this ratio. Viscous forces dominate inertial forces at low Reynolds number. Analytical results have shown that the depletion layer and the interfacial diffusion zone can be depressed as the viscous force becomes significant [3]. There is an advantage in obtaining a relatively higher power density than with a direct methanol fuel cell (DMFC) if hydrogen peroxide is used as both fuel and oxidant [24]. There is also an advantage in that there is no formation of a dioxide like that which occurs in other fuel cells after the reaction of the fuel and the oxidant. Hydrogen peroxide can be easily stored, compared to other fuels, and costs can be reduced because it is possible to fabricate a fuel cell with a simple structure. An oxidation reaction at the anode follows the equation:

$$\begin{aligned} H_2O_2 + OH^- &\rightarrow HO_2^- + H_2O \\ HO_2^- + OH^- &\rightarrow O_2 + H_2O + 2e^- \end{aligned} \quad (1)$$

The chemical reaction of the cathode has the equation:

$$H_2O_2 + 2H^+ + 2e^- \rightarrow 2H_2O \quad (2)$$

Fuel and oxidant were infused into the microfluidic fuel cell by using a syringe pump (KDS200, KD Scientific, USA). Cell performance was measured via the current sweep method using a potentiostat (WEIS500, WonA Tech, Korea). Experiments were conducted by injecting the fuel and oxidant into 20, 30, and 40 mm long microfluidic fuel cells with flow rates of 1000, 1500, 2000, 2500, and 3000 μL min^{-1}.

3. Results and discussion

3.1. Width of electrodes and gap between two electrodes

The Reynolds number is calculated to be about 5.83 when deionized water flows through the designed microchannel at a velocity of 0.1 m s^{-1}. This value is far lower than the maximum Reynolds number, 2100, of laminar flow inside a pipe. Thus, laminar flow is formed in the designed microchannel. When two fluids are infused into the microchannel, laminar flow is obtained, and they flow while bound by the interface without mixing with each other. A diffusion zone occurs around the interface of the two different fluids beside the two laminar flow regions. This diffusion inhibits the interface of the two fluids in the microchannel from efficiently facilitating proton exchange in the fuel cells. This is because fuel crossover happens as a result of diffusion at the interface. This inter-diffusion zone should be considered during the design of the microfluidic fuel cell. The fuel crossover phenomenon, in which an oxidant reacts at the anode and fuel reacts at the cathode, can occur if this diffusion zone expands to the anode and the cathode. Therefore, considering that the inter-diffusion zone directly decreases fuel cell performance, the design of electrode width and spacing between electrodes must be considered a priority.

An analysis domain was set up for the Y-shaped microchannel with two inlets and an outlet, as shown in Fig. 2(a), and the flow pattern was analyzed. Inlets are each 500 μm wide, and the angle between them is 90°. The flow analysis result in Fig. 2(a) is for the case where the electrode length is 40 mm. The left area of the microchannel exhibits a fuel concentration of 100% and a 0% concentration of oxidant. On the contrary, the right area presents a fuel concentration of 0% with 100% oxidant. In the middle of the microchannel, concentrations of the fuel and oxidant change from 0 to 100%. To investigate the diffusion zone around each electrode length in more detail, concentration gradients of fuel and oxidant were inspected at the gate of the channel outlet, as shown in Fig. 2(b). The analyzed results show that the inter-diffusion broadens out naturally since the flow length of the fuel and oxidant becomes longer inside the microchannel as the electrode length increases. When the electrode length is 40 mm, the inter-diffusion is widest, and it exists at points of $y = 0.4$–0.8 mm from the microchannel wall of fuel inlet side. The area in which the electrodes are installed must be where the fuel and oxidant are not diffused in order to prevent the crossover of fuel and oxidant. Based on the analyzed results, the electrode length and the space between the anode and cathode were determined to be 300 and 400 μm, respectively.

3.2. Height of grooves

The groove pattern was fabricated to be a few micrometers to tens of micrometers in the previous micromixer studies, which

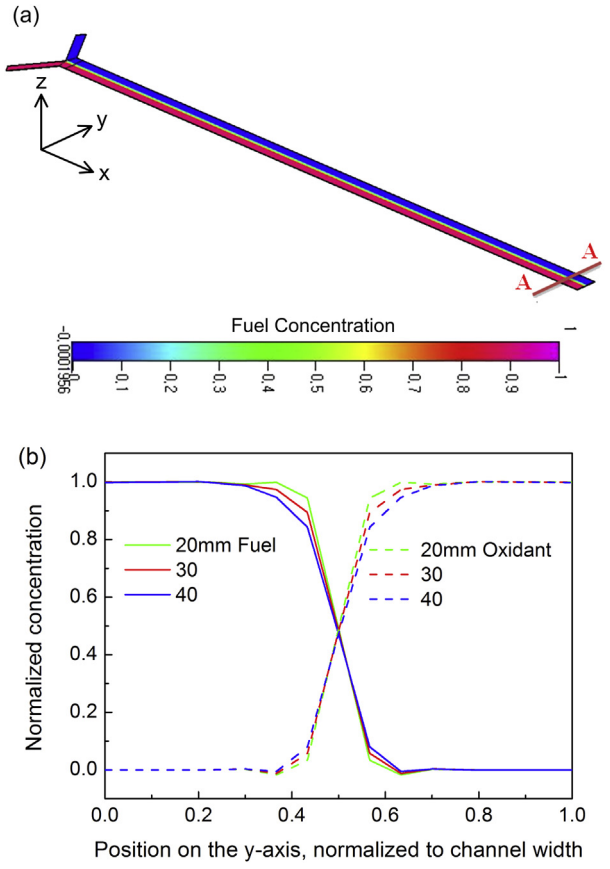

Fig. 2. (a) Inter-diffusion simulation at an electrode length of 40 mm and (b) fuel and oxidant concentration along the A–A direction for 20, 30, and 40 mm long electrodes.

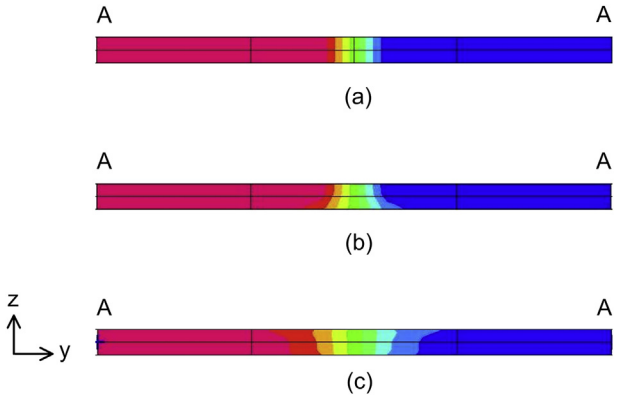

Fig. 3. Section view of concentration simulation results at an electrode length of 40 mm for (a) a planar electrode, (b) a grooved electrode with 0.1-μm high grooves, and (c) grooved electrode with 25-μm high grooves.

used herringbone ridges to effectively mix more than two fluids. When chaotic flow occurs in the microchannel with a groove pattern, the two fluids diffuse normally and more actively at the interface, or they are mixed with each other. Fuel and oxidant mixing indicates that fuel with a positive charge at the anode is also brought into the cathode. This phenomenon is identical to that of the fuel crossover phenomenon in typical fuel cells. Therefore, an objective of this study is to produce chaotic flow over the electrodes with the requirement that fuel crossover does not take place. Flow analysis was performed in order to investigate the influence of the presence of the groove patterns and of the height of the grooves on the flow phenomena in the microchannel and on the electrode surfaces.

The groove angle relative to the direction of fluid flow direction is 45°, which is the same as that in a typical herringbone ridge mixer. Groove widths and the gaps between the grooves are all 200 μm. The conditions for the analysis were simplified into three cases: no groove patterns over the 0.1 μm high electrodes, 0.1 μm high groove patterns over electrodes of the same height, and 25 μm high groove patterns over the electrodes. A height of 0.1 μm is the usual deposition height when the metal film electrodes are fabricated via the semiconductor process, and 25 μm is half the size of the designed microchannel height of 50 μm.

An analysis of the cross-sectional shape is shown in Fig. 3 in the *z*-axis direction (height) just before the outlet of the microchannel (Fig. 2, A–A). The results with respect to the 40.0 mm long electrode indicate that the inter-diffusion zone becomes wider downstream of the microchannel when groove patterns exist on the electrodes. The left region of the microchannel shows only fuel flow, while only oxidant flows in the right region. The middle part represents the region mixing by diffusion. The width of the mixing region increases significantly as the height of the groove patterns increases compared to that of the flat electrodes. The width of the inter-diffusion zone stays almost the same from the top to the bottom of the microchannel for the flat electrodes. For the electrodes with groove patterns, on the other hand, the mixing region is not uniform in the direction of the *z*-axis of the microchannel.

The flow velocity of the fuel was analyzed at the surface of the electrode with respect to the *z*-axis of the microchannel to better

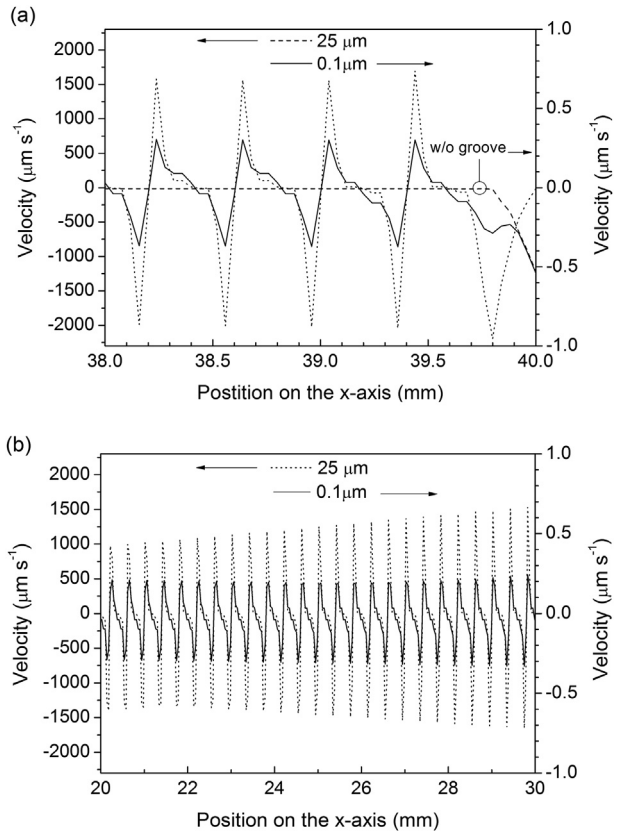

Fig. 4. The calculated *z*-axis velocity component of the fuel at a surface of 0.1- and 25-μm deep grooves and flat anodes in (a) $x = 38–40$ mm and (b) $x = 20–30$ mm, where the electrode length is 40 mm.

comprehend the flow pattern above the electrode. The position analyzed was at the middle of the anode ($y = 150$ μm) and ran from the beginning to the end with respect to the x-axis (length) of the microchannel. The results of the downstream portion at $x = 38$–40 mm from the starting point of the microchannel are shown in Fig. 4(a). In the case of the flat electrode, the flow velocity of the fuel in the direction of the z-axis is zero at the electrode surface, but in the case of the grooved electrode, the velocity in the z-axis changes with alternating positive or negative values. This means that the flow at the electrode surface is upward or downward in turn. Thus, mixing between the depletion zone of the electrode surface and the fuel zone above can be produced just by flowing the fuel through the microchannel when groove patterns are present on the electrode surface. In Fig. 4(a), it can be seen that the flow velocity in the direction of the z-axis is almost 1000 times faster when the groove patterns are 25 μm high than when they are 0.1 μm high.

The variation in the z-axis velocity component of the fuel direction at the midstream portion of the microchannel is shown in Fig. 4(b) with respect to the direction of the x-axis (length) of the microchannel. As shown, the absolute value of the velocity in the z-axis direction at the surface of the electrode increases as it approaches the outlet of the microchannel, even though its growth rate is not uniform. Therefore, the depletion zone and the fuel zone above are mixed more actively as the length of the electrode increases.

Thus, if the groove patterns are 0.1 μm high (similar to the thickness of the electrode) chaotic flow can occur effectively only at the electrode surface because the grooves are not too high. This can also reduce the thickness of the fuel depletion zone without broadening the inter-diffusion zone compared to that with the non-grooved microchannel. Hence, electrodes with 0.1-μm high groove patterns were used in the microfluidic fuel cell.

3.3. Flow pattern observation and performance evaluation with respect to flow rate variation

Before measuring the current density of the fabricated microfluidic fuel cells, whether or not laminar flow occurred under various flow rates was checked. This check was carried out using a microfluidic chip fabricated by bonding a PDMS microchannel layer to a bare glass substrate. Deionized water and blue ink were injected into each of the two inlets at four flow rates of 100, 500, 1,000, and 1500 μL min^{-1}. It was observed that laminar flow formed well at these flow rates.

Then, the flow inside the microchannel was observed at flow rates of 100, 500, 1,000, 1500 μL min^{-1} when fuel and oxidant were introduced into the microfluidic fuel cell with a flat electrode. A

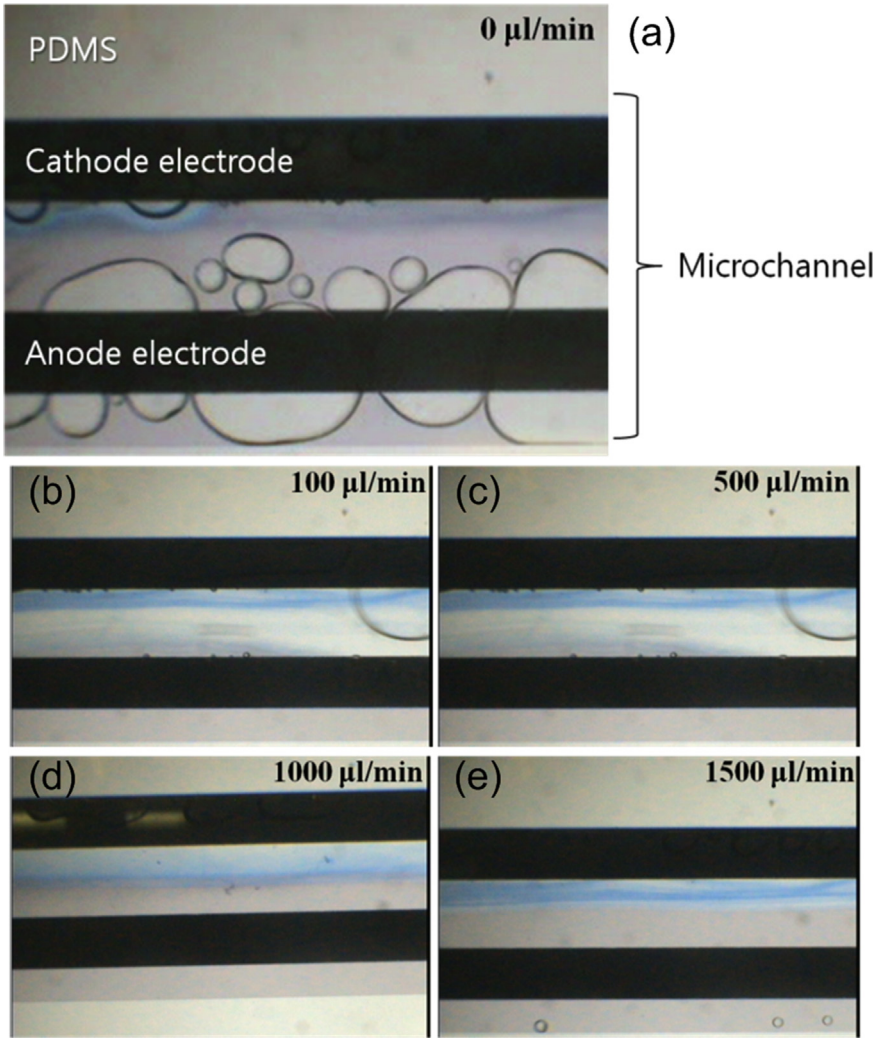

Fig. 5. Photograph of microchannels with fuel and oxidant flow at a flow rate of (a) 0, (b) 100, (c) 500, (d) 1000, and (e) 1500 μL min^{-1}.

solution composed of 0.75 M H_2O_2 and 0.75 M NaOH was injected into the anode, and a solution of 0.75 M H_2O_2 and 0.375 M H_2SO_4 was injected into the cathode. Direct observation was, however, difficult because the solutions are transparent and have no color. Hence, blue ink was added to the H_2O_2 and H_2SO_4 solution.

An image wherein the syringe pump was stopped after the fuel and oxidant were injected at same flow rate and the two flows became steady-state flow is shown in Fig. 5. In the picture, the black portions are platinum electrodes. The microchannel is as indicated in the figure, and the fluids flow from left to right in the picture. Bubble generation was observed at the anode. Seeing that the area of the bubbles increases as time goes by, this would indicate a reaction between the injected fuel and the platinum electrode. Oxygen evolves at the anode according to the chemical reaction in Eq. (1). Relatively fewer bubbles were generated at the cathode as compared to the anode. As the flow rate increased, the bubbling decreases at the anode and at the cathode. It was observed that the generated bubbles escaped through the outlet without remaining at the electrodes at high flow rates. For flow rates less than 1000 mL min^{-1}, current measurement became unstable, and the measured values fluctuated. Shyu et al. [25] observed that interfacial mixing at interface of the two streams was enhanced with bubble generation. Simulations showed that the fuel depletion increases and reaction kinetics of the reaction fluids deteriorate because the supply of fuel and oxidant and the discharge of reaction products are hindered by the existence of bubbles [26]. In the case where hydrogen peroxide was supplied to a platinum electrode, bubble generation was inhibited at a flow rate more than 1000 mL min^{-1} because the rate of the solubility of oxygen gas was larger than the rate of gas generation as the flow rate increased [25]. Consequently, fuel cell experiments in this study were executed with flow rates of 1000, 1500, 2000, 2500, and 3000 μL min^{-1}.

The results of the fuel cells are shown in Fig. 6 for grooved electrodes according to fuel and oxidant flow rates when the electrodes are 30 mm in length. Here, 0.75 M H_2O_2 and 0.75 M NaOH was used as fuel, and the oxidant was 0.75 M H_2O_2 and 0.325 M H_2SO_4. Peak current density and maximum current density show an increasing trend with increasing injection velocity, and the cell potential was stable. This is the same as the results with a general microfluidic fuel cell with a flat electrode [27]. The effect of the oxygen bubbles seems especially significant in the grooved electrode. Bubbles generated were discharged quickly from the microchannel as the injected flow rate increased. This phenomenon was a factor in increasing the contact ratio of the fuel and oxidant to the electrode, which may increase current density. As the flow rate increased from 1500 to 2000, 2500, and 3000 μL min^{-1}, peak current density increased from 2.32 to 2.45, 2.56, and 2.59 mW cm^{-2}, respectively, in the flat electrode, and peak current density increased from 2.52 to 2.68, 2.75, and 2.80 mW cm^{-2}, respectively, in the grooved electrode. This corresponds to improved rates of the peak current density of the grooved electrodes of +8.62, +9.39, +7.42, and +8.0% at flow rates of 1500, 2000, 2500, and 3000 μL min^{-1}, respectively. Thus, the effect of the grooved electrodes appears to be almost unaffected by the change in the flow rate. This could be because the depletion zone is sufficiently recharged by the fuel stream with an increase in the flow rate regardless of whether it happens with or without a grooved electrode [7].

3.4. Performance analysis according to fuel concentration

The current density variations with fuel concentration were obtained experimentally when the electrode was 30 mm in length and the flow rate was 1500 μL min^{-1}. The results with respect to the grooved electrodes are shown in Fig. 7. It has been reported that, in the general flat electrode, the current density increases with a rise in fuel concentration [27]. According to the experimental results, the peak current density of the flat electrode increases to 1.61, 2.12, and 2.32 mW cm^{-2}, and peak current density of the grooved electrode increases to 1.75, 2.27, and 2.52 mW cm^{-2}, as the fuel concentration rises to 0.25, 0.5, and 0.75 M, respectively. This shows that the peak current density improved by 8.7, 7.08, and 8.62%, respectively, due to the grooves in the electrode surface. Further, the change in fuel concentration has no effect on the current density of the grooved electrodes. The improvement in the current density with changes in fuel concentration is due to the increase in mass transfer. Therefore, the effect of the surface of the grooved electrode on reactant transport seems to be marginal.

3.5. Variation in the effect of the grooved electrode according to electrode length

The influence of the length of the electrode on the fuel cell was investigated with a grooved electrode through a comparison of results of experiments with electrodes 20, 30, and 40 mm in length. The cell potential and power density is shown in Fig. 8 for the flat and grooved electrodes when the flow rates of the fuel and oxidant are all 2500 μL min^{-1} and 0.25 M hydrogen peroxide was employed as a fuel. The maximum current density and peak power density

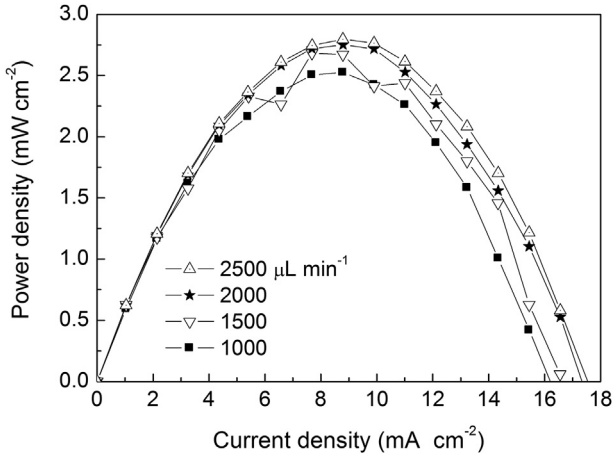

Fig. 6. Power density curve of a grooved electrode microfluidic fuel cell for various flow rates at an electrode length of 30 mm and a fuel of 0.75 M H_2O_2.

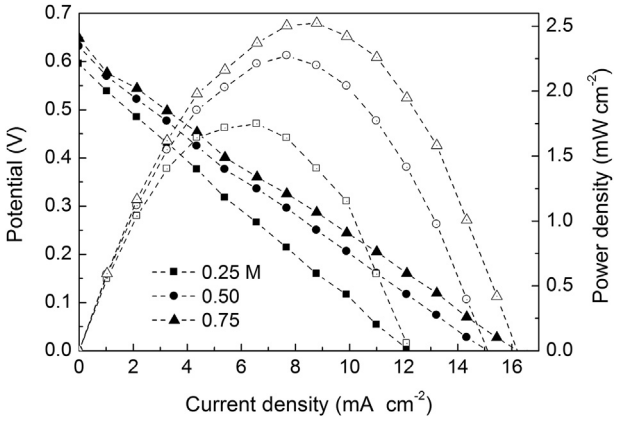

Fig. 7. Polarization and power density curves of grooved electrode microfluidic fuel cell for various fuel concentrations at an electrode length of 30 mm. Flow rate: 1500 μL min^{-1}.

decrease with a lengthening of the electrode. As the electrode becomes 20, 30, or 40 mm long, the peak power density decreases to 3.08, 2.04, and 1.22 mW cm^{-2}, respectively, in the flat electrode, and to 3.12, 1.97, and 1.39 mW cm^{-2}, respectively, in the grooved electrode. This indicates that, as the electrode surfaces are patterned with grooves, the peak power density is augmented in each by +1.30, −3.43, and +13.93%, respectively, for the 20, 30, and 40 mm long electrodes. As the electrode length increases to 40 mm, the augmentation ratio of the peak power density of the electrode with a grooved surface shows an increasing trend.

The power density decreases as the electrodes become longer because the fuel depletion zone thickens toward the outlet from the inlet of the microchannel [28]. Aside from that, the cause of the reduction in power density is the bubbles produced from the reaction of hydrogen peroxide at the platinum electrode surface, as these disturb the flow of the fuel and the oxidant. As the electrode becomes longer, the bubbles perturb the micro-flow inside the microchannel over a larger area of the electrode surfaces. This hinders the catalysis of the platinum electrode, and the bubbles increase the width of the diffusion zone formed at the interface between the fuel and oxidant. It is thus speculated that as electron generation declines, partial fuel cross-over occurs, and finally performance of the fuel cell deteriorates as the electrode becomes longer.

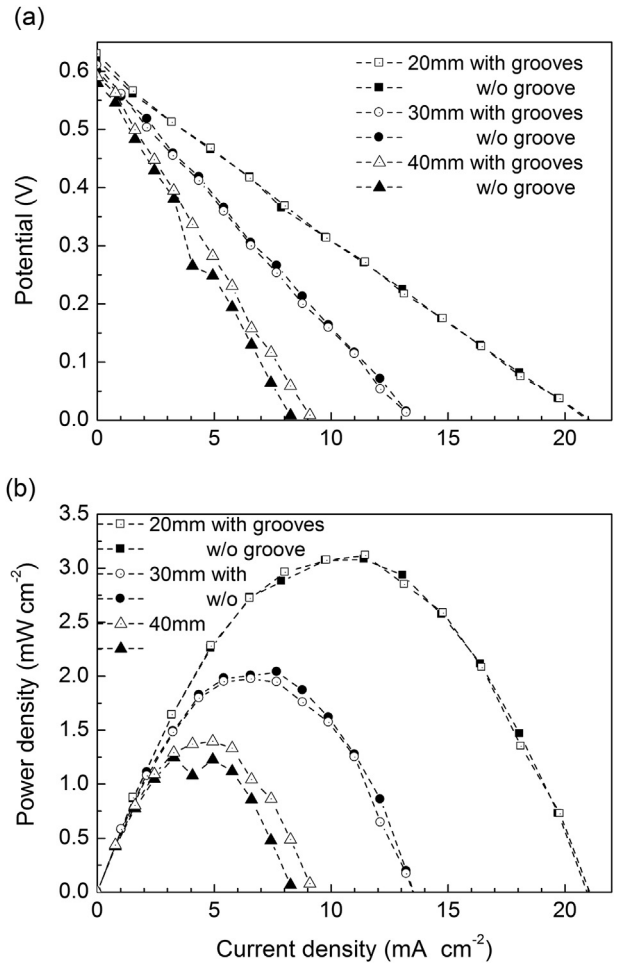

Fig. 8. (a) Polarization and (b) power density curves of microfluidic fuel cells for various lengths of the electrode. Flow rate: 2500 μL min^{-1}. Fuel was 0.25 M H_2O_2 in 0.25 M NaOH. Oxidant was 0.25 M H_2O_2 in 0.125 M H_2SO_4.

In the 20 and 30 mm long electrode, it was confirmed that the existence of a grooved surface on the current density of the fuel cell is not significant. Furthermore, there are instances where the current density and the power density increase in the fuel cell with grooved electrodes. This may be because the fuel and oxidant react and are emitted before the grooved surface takes effect because the electrode is too short. Since the produced bubbles are not discharged well in the grooved electrode as opposed to the flat electrode, the current density of the fuel cell of the grooved electrode could be diminished. If the bubbles are not removed well, the time that the bubbles stay at the electrodes increases. This would effectively reduce the area and the time where fuel and oxidant react with the surface of the electrode.

In general, the current density and power density of microfluidic fuel cells are measured to be high at the grooved electrode rather than at the flat electrode when the electrode length is 40 mm. This is a result of the fact that the fuel depletion zone shrinks because the grooved pattern induces chaotic flow normal to the electrode surface. Furthermore, this effect increases with longer electrodes, as was shown in the simulation. This may also be an outcome of the reactivity of the fuel and oxidant with the platinum electrodes, which is enhanced because the surface area of the grooved electrode is larger than that of the flat electrode. Therefore, the grooved electrode has a great effect for long electrodes, where the fuel depletion zone thickens and its influence is high. In this study, the maximum rate of increase of the peak power density as a result of the groove patterning is 13.93%, which is not as good as the 25% achieved through a separated layout configuration of the electrodes [10] and the 10–40% achieved by a passive micromixer with a herringbone ridge pattern [8]. Research is underway to find the optimum groove angle and pattern shape, which can further improve the power density.

4. Conclusions

Grooved electrodes are used to reduce the depletion boundary layer in order to enhance the performance of the microfluidic fuel cell. Performance is improved since the fuel depletion zone existing over the electrodes is attenuated by the micro-flows that occur as a result of the grooved pattern on the electrode surface. The increased surface area of the grooved electrodes (when compared to that of the planar electrode) also helps to improve the performance of the fuel cell because the reactivity of the fuel and the oxidant with the electrode increases. This study has significance in that power density can be improved with only shape modification of the electrode surface regardless of the type of fuel, oxidant, and electrode materials used. It is confirmed that this is a main factor in enhancing the performance of the microfluidic fuel cell.

Performance improvements in the microfluidic fuel cell are examined with grooved patterns by comparing the performance and efficiency of the fuel cell with respect to the changes in electrode length, fuel concentration, and flow rate. The power density and current density of the microfluidic fuel cell of the grooved electrode also show an increasing tendency, as with the flat electrode. With flow rates in the range of 1000–3000 μL min^{-1}, the influence of the flow rate on the efficacy of the grooved pattern appears to be tenuous. When the electrode length is short, such as 20 or 30 mm, it is observed that the existence of a grooved pattern does not have a great effect on the current density and power density of the fuel cell. On the contrary, the current density of a microfluidic fuel cell is measured to be larger for the microfluidic fuel cell integrated with a grooved electrode than that with a flat electrode in the case of the 40-mm long electrodes. This is because the fuel depletion zone is effectively diminished. Hence, the grooved electrode with a longer length is helpful in a case where

fuel must be supplied at a high flow rate because a large amount of power is required for a short time. Further, convenient fabrication processes can take advantage of the planar structure of the electrode.

In this study, hydrogen peroxide-based fuel and oxidant are employed in a microfluidic fuel cell with platinum electrodes. Power density is enhanced if hydrogen peroxide is employed as compared with other solutions. Bubbles appear at the electrode surface from the reaction with the platinum, though, and these make analysis of the performance of the microfluidic fuel cell difficult. In the future, a more detailed study should be conducted to provide effective analysis of the grooved pattern by employing a fuel and oxidant that produce no bubbles even when using a platinum electrode or when using an electrode where no bubbles are generated through the use of a hydrogen peroxide solution.

Acknowledgements

This research was supported by the Basic Science Research Program through the National Research Foundation of Korea (NRF) funded by the Ministry of Education, Science and Technology (NRF-2012R1A1A2009264).

References

[1] J. Yang, S. Ghobadian, P.J. Goodrich, R. Montazami, N. Hashemi, Phys. Chem. Chem. Phys. 15 (2013) 14147–14161.
[2] R. Ferrigno, A.D. Stroock, T.D. Clark, M. Mayer, G.M. Whitesides, J. Am. Chem. Soc. 124 (2002) 12930–12931.
[3] E.R. Choban, L.J. Markoski, A. Wieckowski, P.J.A. Kenis, J. Power Sources 128 (2004) 54–60.
[4] R.S. Jayashree, L. Gancs, E.R. Choban, A. Primak, D. Natarajan, L.J. Markoski, P.J.A. Kenis, J. Am. Chem. Soc. 127 (2005) 16758–16759.
[5] E. Kjeang, B.T. Proctor, A.G. Brolo, D.A. Harrington, N. Djilali, D. Sinton, Electrochim. Acta 52 (2007) 4942–4946.
[6] W. Sung, J.-W. Choi, J. Power Sources 172 (2007) 198–208.
[7] S.A.M. Shaegh, N.-T. Nguyen, S.H. Chan, Int. J. Hydrogen Energy 36 (2011) 5675–5694.
[8] S.K. Yoon, G.W. Fichtl, P.J.A. Kenis, Lab. Chip 6 (2006) 1516–1524.
[9] E. Kjeang, N. Djilali, D. Sinton, J. Power Sources 186 (2009) 353–369.
[10] K.G. Lim, G.T.R. Palmore, Biosens. Bioelectron. 22 (2007) 941–947.
[11] S.A.M. Shaegh, N.-T. Nguyen, S.H. Chan, W. Zhou, Int. J. Hydrogen Energy 37 (2012) 3466–3476.
[12] D. Fuerth, A. Bazylak, J. Fluids Eng. Trans. ASME 135 (2013) 021102.
[13] A.D. Stroock, S.K.W. Dertinger, A. Ajdari, I. Mezic, H.A. Stone, G.M. Whitesides, Science 295 (2002) 647–651.
[14] P.B. Howell Jr., David R. Mott, S. Fertig, C.R. Kaplan, J.P. Golden, E.S. Oran, F.S. Ligler, Lab. Chip 5 (2005) 524–530.
[15] H.-Y. Wu, C.-H. Liu, Sens. Actuators A Phys. 118 (2005) 107–115.
[16] J.-T. Yang, K.-J. Huang, Y.-C. Lin, Lab. Chip 5 (2005) 1140–1147.
[17] D.G. Hassell, W.B. Zimmerman, Chem. Eng. Sci. 61 (2006) 2977–2985.
[18] J.B. Knight, A. Vishwanath, J.P. Brody, R.H. Austin, Phys. Rev. Lett. 80 (1998) 3863–3866.
[19] L.H. Lu, K.S. Ryu, C. Lin, J. Microelectromech. Syst. 11 (2002) 462–469.
[20] S.Z. Qian, J.Z. Zhu, H.H. Bau, Phys. Fluids 14 (2002) 3584–3592.
[21] A.O.E. Moctar, N. Aubry, J. Batton, Lab. Chip 3 (2003) 273–280.
[22] C.-H. Cho, W. Cho, Y. Ahn, S.-Y. Hwang, J. Micromech. Microeng. 17 (2007) 1810–1817.
[23] M.D. Cruz, J.M. Siquerios, J. Valenzuela, R. Machorro, J.J. Portelles, A. Fundora, Ferroelectrics 225 (1999) 319–325.
[24] S. Hasegawa, K. Shimotani, K. Kishi, H. Watanabe, Electrochem. Solid State Lett. 8 (2005) A119–A121.
[25] J.-C. Shyu, C.-S. Wei, C.-J. Lee, C.-C. Wang, Appl. Therm. Eng. 30 (2010) 1863–1871.
[26] J. Peng, Z.Y. Zhang, H.T. Niu, Fuel Cells 12 (2012) 1009–1018.
[27] J.-C. Shyu, C.-L. Huang, T.-S. Sheu, H. Ay, Micro Nano Lett. 7 (2012) 740–743.
[28] I.B. Sprague, D. Byun, P. Dutta, Electrochim. Acta 55 (2010) 8579–8589.